SCAL IMPORTANCE AND CHALLENGES FOR AN INTEGRATED PETROPHYSICAL EVALUATION OF THE RAU DISCOVERY

Kåre Langaas[1,3], Stefano Pruno[2] and Petter Gahre[1]
1) Norwegian Energy Company ASA, 2) Weatherford Laboratories AS, 3) Now at Marathon Oil Norge AS

This paper was prepared for presentation at the International Symposium of the Society of Core Analysts held in Aberdeen, Scotland, UK, 27-30 August, 2012

ABSTRACT
Rau is a Danish oil discovery, within the Ty formation, of Paleocene age. The main challenges and results of a SCAL program are presented. The paper gives a case study of how to build a SCAL based saturation-height model and how to best integrate this with the other petrophysical data.

INTRODUCTION
Rau, situated west of the producing Cecilie and Siri oil fields, was discovered in 2007. The main reservoir is the Ty formation of Paleocene age. The sandstone has a complex lithology and pore structure, characterized by the presence of various minerals and clay components (mainly glauconite, illite and smectite). One of the four well penetrations was cored, using oil based mud. One of the key uncertainties during the evaluation phase of the discovery was the water saturation. Dean Stark (DS) analysis was performed as part of the conventional core analysis program. These measurements were interpreted as being uncertain, linked to the fact that the DS plugs were cut onshore 25 days after the coring offshore. The main objective of the SCAL program was to reduce the uncertainty in the water saturation.

SCAL PROGRAM CHALLENGES AND RESULTS
A key part of the SCAL program was the porous plate capillary pressure measurements, with associated resistivity index measurements. These were performed at pseudo reservoir conditions, applying a realistic net confining pressure (NCP) and temperature. Laboratory oil and synthetic brine were the fluids used. Glauconite bearing sandstones present specific challenges with respect to core handling and preparation, prior to the SCAL experiments [1]. Great care was given to the SCAL preparation process and experimental procedure. The selected plugs were cleaned using low rate miscible solvents flooding, in a core holder at 60^{o} C. Prior to the capillary experiment, synthetic formation brine was flowed through the samples to ensure full saturation. Sample resistivity, and brine volume displaced during the experiment were monitored until stabilization was achieved, indicating the plug was at both ionic and capillary pressure equilibrium. An example of the results is presented in Figure 1 and Figure 2 for a single plug sample. The average Archie exponent *n* measured is 2.2 while the high water saturation part of the

curve has a lower *n* value (around 2.0). This variation in *n* can be explained by glauconite presence [1]. Mercury injection capillary pressures (MICP) measurements were performed on cleaned end trims from the SCAL plugs and the Dean Stark plugs.

SCAL BASED SATURATION HEIGHT FUNCTION

A general saturation height model contains both an irreducible water saturation (S_{wirr}) part and a "mobile" water saturation (S_{wmob}) part. The term "mobile" is used since this water can be mobilised if the viscous forces are higher than the capillary forces trapping this water within the transition zone. We assume that

$$S_w(RT,k,h) = S_{wirr}(RT,k) + S_{wmob}(RT,k,h) \ , \quad (1)$$

where RT is the rock type, k is the permeability and h is the height above the free water level (FWL).

Irreducible Water Saturation Model

Figure 1 shows an oil-water porous plate drainage example (red curve). The water saturation is close to an asymptotic value at 12 bar capillary pressure. A 12 bar capillary pressure corresponds to 350 m above the FWL. Figure 3 shows the MICP results from the end trim of the same SCAL plug. The MICP shows a micro-pore entry pressure most easily picked via the derivative or second derivative [2]. (The theoretical derived pore throat radius at this point is just below 0.1e-6 m). This entry pressure is around 13 bar when converting from an air-Hg system to an oil-brine system. The assumption used here is that oil will never enter these micro-pores and that these data points can be used in a S_{wirr} model [2]. In Figure 3 the mercury saturation is calculated using the MICP porosity (i.e. assuming that all pore space is filled). In the below analysis we have used the end trim's He-measured porosity as basis for S_{wirr}. A total of 28 MICP end trims were analyzed and all showed a micro-pore entry level between 8 and 15 bar oil-brine (converted) capillary pressure. Figure 4 shows these S_{wirr} estimates vs. the measured core depth. Also shown is the porous plate water saturations at 12 bar capillary pressure. Both a chlorite cemented and a calcite cemented region is indicated within the figure. An upper zone with high permeability sand is present with relatively high S_{wirr} estimates. This is shown even clearer in Figure 5 when plotting the same data vs. permeability (MICP based theoretical permeability [3] for the MICP plugs, Klinkenberg corrected air permeability at 20 bar NCP for the SCAL plugs). The chlorite and calcite cemented zones seem to follow the common trend of the data, whilst the upper high permeability sand shows a different relationship. An overall trend is weighted towards the SCAL plugs as these include the NCP effect.

"Mobile" Water Saturation Model

Figure 6 shows the MICP and porous plate data (excluding chlorite and calcite cemented samples) scaled as a J-function [4]

$$J = \sqrt{\frac{k}{\phi}} \frac{P_c}{\sigma \cos\theta} \tag{2}$$

where k is the MICP permeability or Klinkenberg corrected air permeability, ϕ is the He based porosity, σ is the interfacial tension and θ is the contact angle. Normalized water saturation

$$S_{wn} = (S_w - S_{wirr}) / (1 - S_{wirr}) \tag{3}$$

is used in the plot. The sand plugs are close to having a common J-functionality. To make a "mobile" water model a lambda function [5] is fitted to the data

$$J = cS_{wn}^{-1/\lambda} \tag{4}$$

where c and λ can be seen as fit parameters. The SCAL plugs are given most weight in the fit. It is key that the lambda function match the interval corresponding to the oil column. Combining equation (2) and (4) we get

$$P_c = c\sigma\cos(\theta)\sqrt{\frac{\phi}{k}} S_{wn}^{-1/\lambda} \tag{5}$$

The capillary pressure needs to balance the gravity head of the water-oil density difference $\Delta\rho$ above the FWL

$$P_c = \Delta\rho g h \tag{6}$$

Combining equations (5) and (6) and solving using equation (3) we arrive at the saturation height function

$$S_w = S_{wirr} + (1 - S_{wirr}) \left[\frac{\Delta\rho g h \sqrt{\frac{k}{\phi}}}{c\sigma\cos\theta} \right]^{-\lambda} \tag{7}$$

SCAL – PETROPHYSICS INTEGRATION

The derived saturation height function was tested in the petrophysical (log) domain, firstly within the cored well, where the core permeability (Klinkenberg corrected air permeability) and core porosity was used in the model. The result is shown in Figure 7 (left panel w saturation data). The points are the Dean Stark water saturations, the black and red lines are two alternative log based water saturations (based on n=2.1 and a rock-variable n approach), the thin and bold blue lines are the SCAL based S_{wirr} and S_w model result, respectively. Some comments are in place linked to letters in the figure: a) Chlorite cemented section where the SCAL based model gives 100% water; this is linked to the lambda fit only being based on good quality sands. A refinement by making a separate J-fit for this rock type is needed to improve the match. b) & c) Areas where the "top sand" irreducible water saturation model was applied which gives a good match to the other data. b) A small interval where the SCAL based model indicates an upside that correlates with several smaller calcite cemented zones that impact the resistivity. (Seen in the core data, but also seen via the rapidly changing permeability/MDT data in Figure 7). Overall,

the SCAL based model supports the log interpretation based on n=2.1 more than the alternative rock variable n approach.

Next, the model is applied on a non-cored well that had a NMR-derived permeability (KTIM) estimate. Figure 8 (middle track) shows the NMR permeability as the orange curve (partly hidden behind the black curve). Also shown are the MDT drawdown mobilities, which are good in situ permeability indicators. The right track is the effective porosity log used in the model. By comparing the NMR permeability with the MDT drawdown mobility, a different ratio is seen in zone a). This may indicate chlorite cementation in this zone that results in a lower permeability/porosity ratio, not detected by the NMR. Hence, the permeability in this zone was adjusted to keep the permeability/MDT mobility ratio the same as the lower zone. This corrected NMR based permeability (black line in middle track) was then used in the model. The model result is seen in the left track, where the thin and bold blue lines are the SCAL based S_{wirr} and S_w model result, respectively. The result is also for this well close to the n=2.1 based log interpretation of S_w. One important point for this type of material is that the n value changes with saturation/capillary pressure [1], (Figure 2). The rock-based variable-n log (black line in left track of Figure 7 and Figure 8) is based on a constant n-value per RT using the trend value. This matched the Dean Stark data well. However, the capillary pressure in the top of the oil column in Figure 7 and Figure 8 is only around 0.6 bar. Hence, it could be more correct to use the n-values linked to lower capillary pressure values. This again is supporting the n=2.1 interpretation more than the rock-variable n approach.

CONCLUSION

Reservoirs with complex lithology and pore structures characterized by the presence of various minerals and clay components give extra challenges for the planning and integration of SCAL data. A thorough SCAL based saturation height model helped the petrophysical interpretation of Rau, with respect to rock type subdivision, permeability and water saturation.

ACKNOWLEDGEMENTS

We thank RWE, Nordsøfonden and Noreco for the permission to publish.

REFERENCES

1. Hammervold Thomas, W, Ringen, J.K. and Rasch, S.O "Effect of glauconite on petrophysical properties as revealed by core analysis", paper SCA2003-32 (2003).
2. Høier, C., pers. comm.
3. Swanson, B.F, "A simple correlation between air permeabilities and stressed brine permeabilities with mercury capillary pressures", SPE 8234 (1978).
4. Leverett, M.C, "Capillary behavior in porous solids". *Trans. AIME*, (1941), **142**.
5. Brooks, R.H. and Corey, A.T., "Properties of porous media affecting fluid flow", *J. Irrig. Drain. Div.*, Proc. ASCE, (1966), **92**.

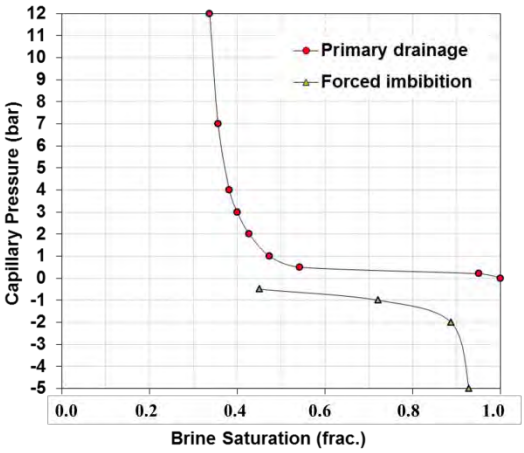

Figure 1: Porous plate capillary pressure for core at depth 2574.88 m

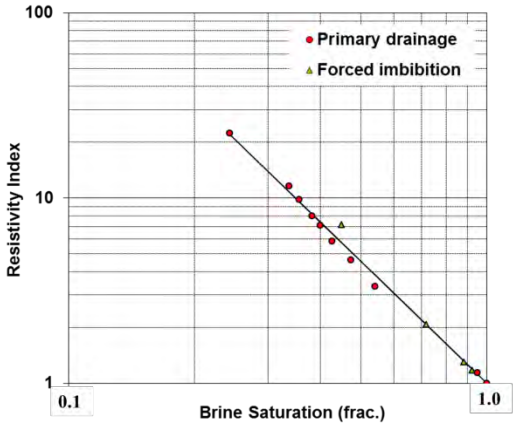

Figure 2: Resistivity index for core at depth 2574.88m

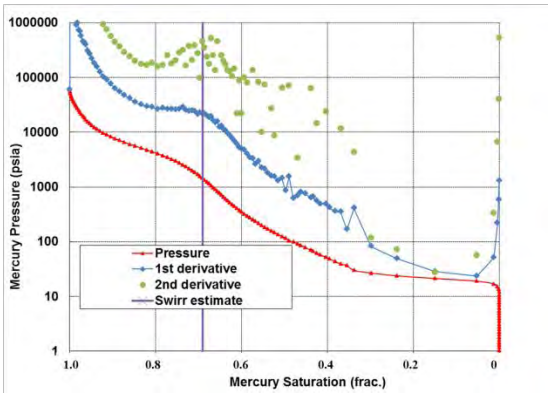

Figure 3: Mercury injection capillary pressure for end-trim of core at depth 2574.88m

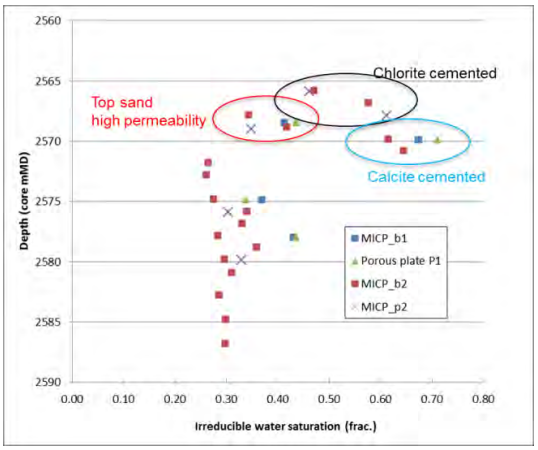

Figure 4: S_{wirr} estimates vs. core depth.

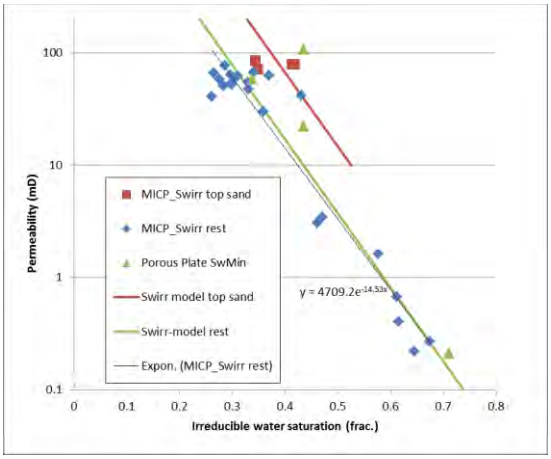

Figure 5: S_{wirr} estimates vs. core permeability.

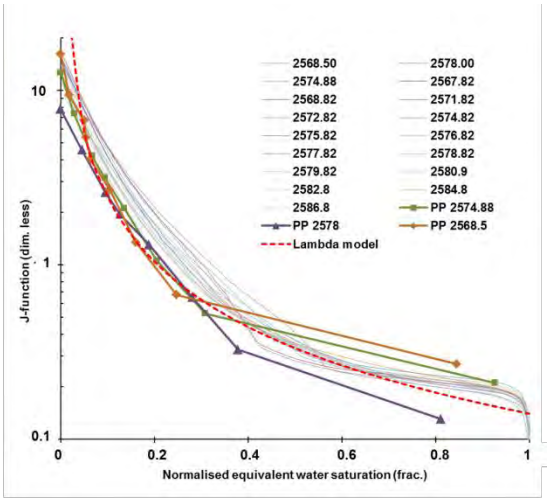

Figure 6: J-functions for all MICP and porous plate (PP) plugs (except calcite and chlorite cemented plugs). Also shown is the Lambda model fit used in the saturation height model.

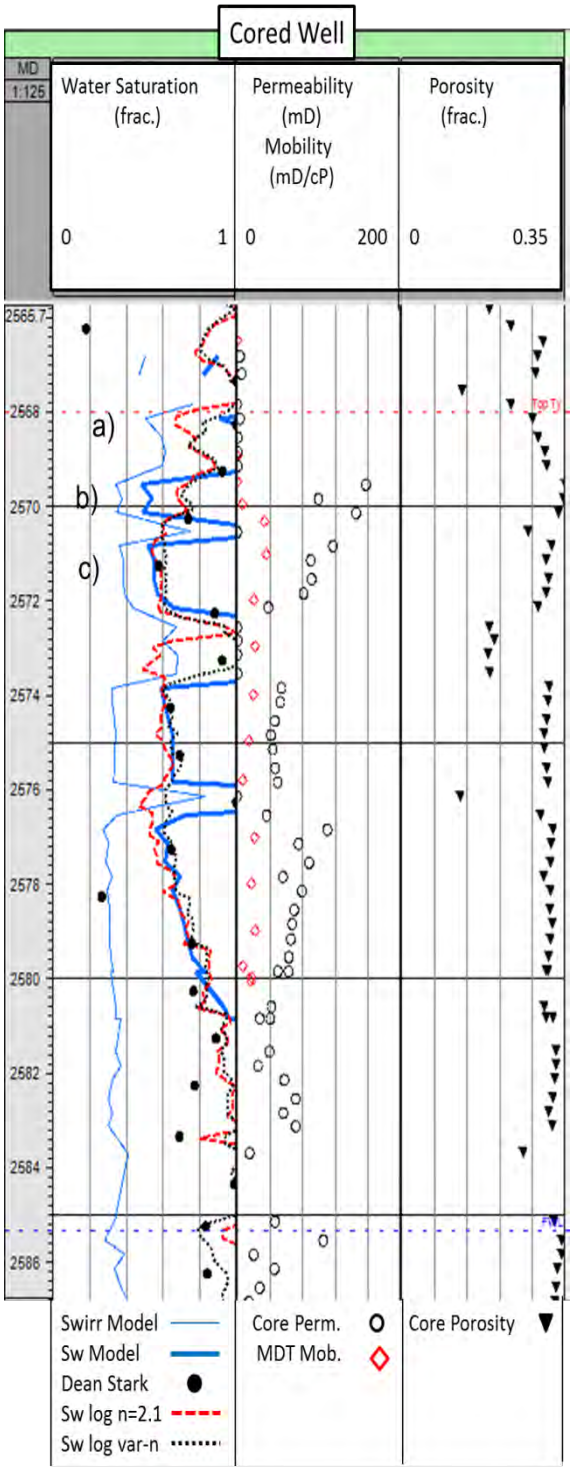

Figure 7: Cored well. Various data and model results vs. measured depth. See text for explanation.

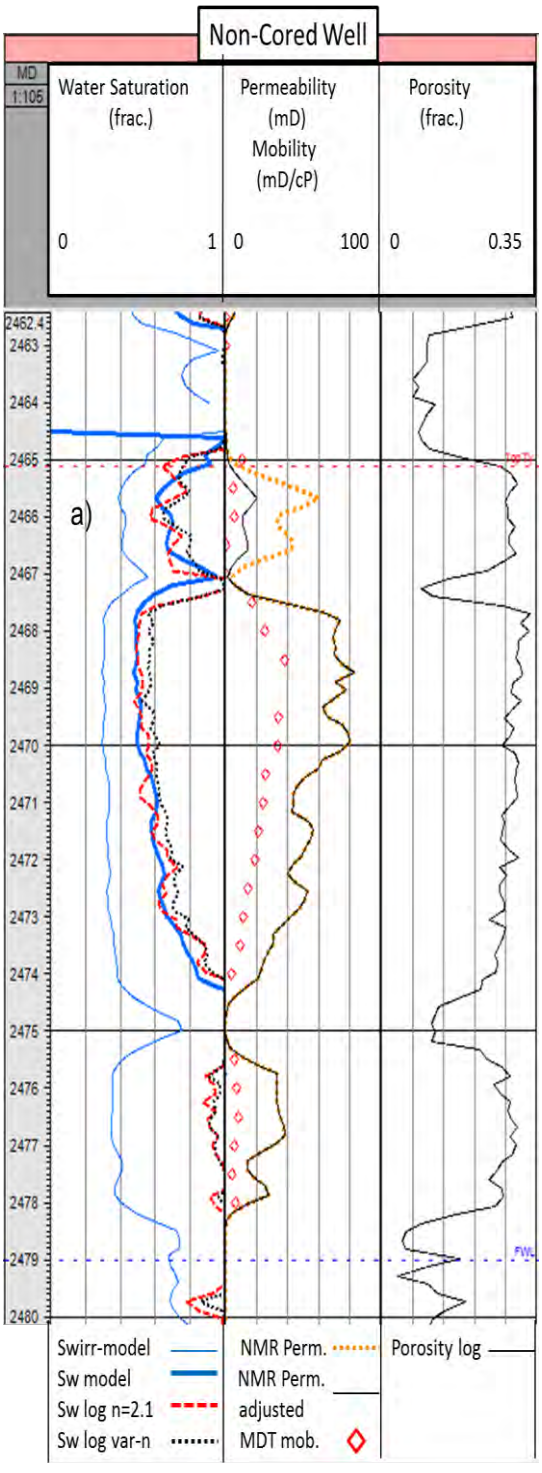

Figure 8: Non-cored well. Various data and model results vs. measured depth. See text for explanation.